Circ J 2003; **67:** 898–900

Intravenous Administration of Nifekalant Hydrochloride for the Prevention of Ischemia-Induced Ventricular Tachyarrhythmia in Patients With Renal Failure Undergoing Hemodialysis

Masafumi Myoishi, MD; Satoshi Yasuda, MD; Shunichi Miyazaki, MD; Kazuyuki Ueno, PhD*; Isao Morii, MD, Kazuhiro Satomi, MD; Yoritaka Otsuka, MD; Atsushi Kawamura, MD; Takashi Kurita, MD; Shiro Kamakura, MD; Hiroshi Nonogi, MD

Excretion in the urine is an important pathway for the elimination of nifekalant hydrochloride (NIF), a novel class III antiarrhythmic agent. Three patients with renal failure were undergoing hemodialysis and receiving NIF for the prevention of ischemia-induced ventricular tachyarrhythmia. Because NIF is not dialyzed, dose adjustment at relatively low concentrations was required, with monitoring of the QT interval. (*Circ J* 2003; **67:** 898–900)

Key Words: Antiarrhythmic agents; Hemodialysis; Ventricular tachyarrhythmia

Nifekalant hydrochloride (NIF) is a novel class III antiarrhythmic agent that is administered intravenously and selectively blocks the rapid component of the delayed rectifier K^+ current.[1] The most significant adverse effect of NIF is QT-interval prolongation with torsades de pointes,[2] which may be dose-related. Because excretion in the urine is an important pathway for its elimination, NIF must be administered cautiously in patients with renal failure. We report 3 patients undergoing hemodialysis (HD) for whom NIF administered at a relatively low dose effectively prevented ischemia-induced ventricular tachyarrhythmia.

Case Reports

Case 1

A 69-year-old man with diabetic nephropathy was hospitalized because of congestive heart failure following acute anterior myocardial infarction. The left ventricular ejection fraction was severely depressed to 33% and the ST segment remained elevated in the V_{1-5} leads. During HD, ventricular tachyarrhythmias (sustained ventricular tachycardia and fibrillation) developed frequently and were difficult to terminate by direct-counter shock and to prevent with conventional medical therapy. Thus, we administered NIF intravenously, at a loading dose of 0.1 mg/kg body weight (BW) and a maintenance dose of 0.2 mg/kg BW/h, which were much lower doses than previously reported (ie, loading dose: 0.30 mg/kg BW; maintenance dose: 0.60 mg/kg BW/h).[3] The ventricular tachyarrhythmias were effectively suppressed by NIF, and the corrected QT interval (QTc) was extended from 0.46 s to 0.57 s as the baseline. Percutaneous coronary intervention was performed on the 75% residual stenosis of the mid-segment of the left anterior descending artery.

Case 2

A 78-year-old man undergoing HD because of diabetic nephropathy was referred for assessment of unstable angina pectoris and ST segment depression that remained symptomatic in the V_{3-5} leads. He also had the complication of sustained ventricular tachycardia, which appeared to be of the incessant form. Intravenous administration of NIF was effective in preventing the ventricular tachycardia at a loading dose of 0.1 mg/kg BW and a maintenance dose of 0.15 mg/kg BW/h, and increased the QTc from 0.45 s as the baseline to 0.48 s. Coronary angiography revealed 90% stenosis in the proximal segment of the left anterior descending artery and 75% stenosis in mid-segment of the left circumflex artery, and a hypoplastic right coronary artery. The left ventricular ejection fraction was 42%. The patient underwent coronary artery bypass grafting as revascularization therapy.

Case 3

A 77-year-old man with chronic glomerulosclerosis undergoing HD had undergone coronary artery bypass grafting 14 years earlier. Only the graft of the left internal thoracic artery to the posterolateral branch was patent and the left ventricular ejection fraction was severely depressed to 21%. He was hospitalized because of acute dyspnea and chest discomfort. Because of high fever, the heart rate increased and then sustained ventricular tachycardia, which was frequently accompanied by hemodynamic collapse (Fig 1A,B). To prevent this life-threatening tachyarrhythmia, NIF was administered intravenously at a loading dose of 0.2 mg/kg BW and a maintenance dose of 0.20 mg/kg BW/h with the prolongation of the QTc (Fig 1C). However, torsade de pointes was newly induced when the QTc exceeded 0.60 s (Fig 1D) and therefore the dosage of NIF

(Received July 1, 2003; revised manuscript received August 1, 2003; accepted August 18, 2003)

*Divisions of Cardiology and *Pharmacology, National Cardiovascular Center, Osaka, Japan*

Mailing address: Satoshi Yasuda, MD, Division of Cardiology, Department of Medicine, National Cardiovascular Center, 5-7-1 Fujishiro-dai, Suita, Osaka 565-8565, Japan. E-mail: syasuda@hsp.ncvc.go.jp

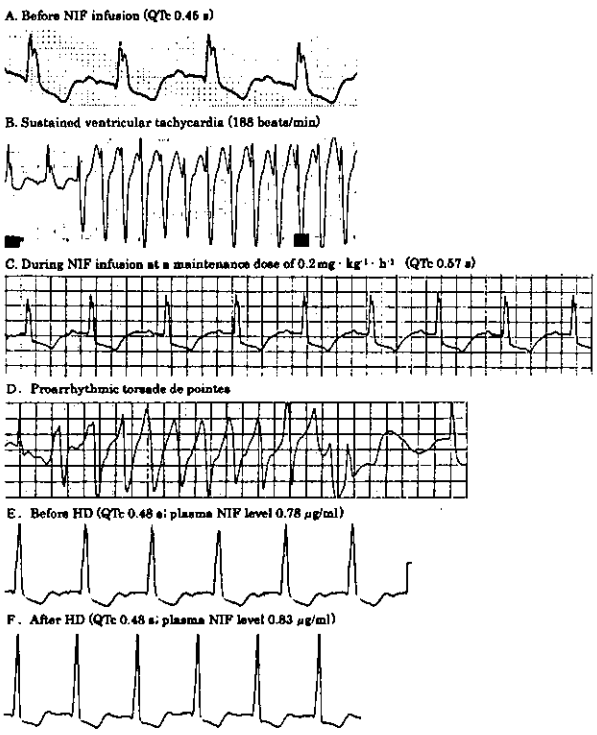

Fig 1. Case 3: ECG recording. (A) Before nifekalant hydrochloride (NIF) infusion (QTc 0.45 s), (B) sustained ventricular tachycardia (188 beats/min) with hemodynamic collapse, (C) during NIF infusion at a maintenance dose of 0.2 mg/kg body weight/h (QTC 0.57 s), (D) proarrhythmic torsade de pointes, (E) before hemodialysis (HD) (QTc, 0.48 s; plasma NIF concentration, 0.78 μg/ml) and (F) after HD (QTc, 0.48 s; plasma NIF concentration, 0.83 μg/ml).

was decreased to 0.15 mg/kg BW/h, minimizing the induction of proarrhythmic adverse events. Coronary angiography revealed the patency of the graft to the posterolateral branch, progression of the left main trunk lesion to 75% stenosis and total occlusion of the right coronary artery, for which the left anterior descending artery was the source of collateral circulation. Coronary artery stenting was performed successfully on the left main trunk lesion protected by the bypass graft.

We also measured the plasma NIF concentration by high-performance liquid chromatography and it did not change significantly before or after HD (Fig 1E,F). In this patient with chronic renal failure, even a relatively low dosage was sufficient to obtain a therapeutic concentration of NIF (≈0.5 μg/ml). Fig 2 shows the relationship between the plasma concentration of NIF and the QTc during continuous infusion of NIF at 0.15 mg/kg BW/h.

Discussion

Cardiovascular mortality is high in patients with chronic renal failure, which may be related in part to ventricular arrhythmias[4] Myocardial ischemia is a potential contributing factor, in association with the rapid changes in the concentrations of electrolytes and in pH that occur during HD. Therefore, antiarrhythmic treatment is very important in patients with renal failure and ischemic heart disease, but because renal failure modifies the pharmacokinetics and pharmacodynamics of drugs, the dosages need to be adjusted[5]

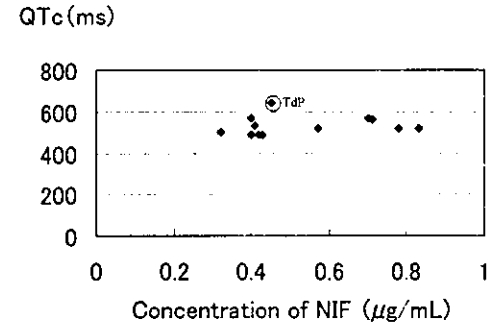

Fig 2. Relationship between nifekalant hydrochloride (NIF) concentration and QTc during continuous infusion of NIF at 0.15 mg/kg body weight/h in case 3. TdP, proarrhythmic torsade de pointes.

Nifekalant hydrochloride is a pure K^+ channel blocker that does not have a β-adrenergic inhibiting effect[1] This unique class III antiarrhythmic agent is a useful emergency intravenous treatment that effectively suppresses refractory ventricular tachyarrhythmias in patients with myocardial ischemia and infarction[2] in which the K^+ channels play a key role[6] Although the kidney is one of the important pathways of elimination of NIF, there is limited information on using NIF in patients with chronic renal failure undergoing HD.

Regarding the pharmacokinetics of NIF, only the unchanged form is active. Its half-life is 1.5 h and the volume of distribution is 0.14 L/kg. The urinary excretion ratio for the unchanged form is approximately 30%. The remaining NIF undergoes glucuronate conjugation in the liver, which may be affected by hemodynamics.

In the present study, taking into account the impaired left ventricular function and the interruption to renal excretion, we administered NIF at dosages that were one-half of those previously used in patients with normal renal function and stable hemodynamics[3] As shown in case 3, continuous infusion of NIF at 0.15 mg/kg BW/h achieved a therapeutic concentration, in the plasma (≈0.5 μg/ml), comparable with administration of 0.25 mg/kg BW/h reported previously in a patient without renal failure[7] We also noted that the NIF concentration did not change significantly before or after HD, even under continuous infusion. Because NIF binds strongly to protein (86–96%, unpublished data), it may not be dialysed.

A serious complication of NIF is torsade de pointes[2] which was transiently induced in case 3 when the QTc extended beyond 0.60 s. However, it was not associated with an elevated blood concentration of NIF, indicating that the dose range for the safe use of NIF may be narrow in patients with renal failure. Therefore, it is important to monitor the QTc in these particular patients and to use a low starting dose in order to minimize the induction of proarrhythmic adverse events.

In conclusion, NIF is an effective emergency intravenous treatment for patients with renal failure undergoing HD. Administration even at relatively low doses achieves a therapeutic concentration sufficient for the prevention of ischemia-induced ventricular tachyarrhythmias.

References

1. Nakaya H, Tohse N, Takeda Y, Kanno M. Effects of MS-551, a new class III antiarrhythmic drug, on action potential and membrane currents in rabbit ventricular myocytes. *Br J Pharmacol* 1993; **109:**

157–163.
2. Takenaka K, Yasuda S, Miyazaki S, Kurita T, Sutani Y, Morii I, et al. Initial experience with nifekalant hydrochloride (MS-551), a novel class III antiarrhythmic agent, in patients with acute extensive infarction and severe ventricular dysfunction. *Jpn Circ J* 2001; **65**: 60–62.
3. Naitoh N, Taneda K, Tagawa M, Furushima H, Yamaura M, Aizawa Y. Electrophysiologic effects of intravenous MS-551, a novel class III antiarrhythmic agent, on human atrium and ventricle. *Jpn Heart J* 1998; **39**: 297–305.
4. Gruppo Emodialisi e Patologie Cardiovasculari. Multicenter, cross-stional study of ventricular arrhythmias in chronically haemodialysed patients. *Lancet* 1988; **2**: 305–309.
5. Talbert RL. Drug dosing in renal insufficiency. *J Clin Pharmacol* 1994; **34**: 99–110.
6. Ehlert FA, Goldberger JJ. Cellular and pathophysiological mechanisms of ventricular arrhythmias in acute ischemia and infarction. *Pacing Clin Electrophysiol* 1997; **20**: 966–975.
7. Shiga T, Ando S, Suzuki T, Matsuda N, Kasanuki H. Reverse use-dependent QT prolongation during infusion of nifekalant in a case of recurrent ventricular tachycardia with old myocardial infarction. *J Electrocardiol* 2001; **34**: 77–80.

Haplotype analysis of *ABCB1/MDR1* blocks in a Japanese population reveals genotype-dependent renal clearance of irinotecan

Kimie Sai[a,b], Nahoko Kaniwa[a,c], Masaya Itoda[a], Yoshiro Saito[a,e], Ryuichi Hasegawa[c], Kazuo Komamura[f,g], Kazuyuki Ueno[h], Shiro Kamakura[f], Masafumi Kitakaze[f], Kuniaki Shirao[i], Hironobu Minami[j], Atsushi Ohtsu[m], Teruhiko Yoshida[k], Nagahiro Saijo[j], Yutaka Kitamura[n,o], Naoyuki Kamatani[n], Shogo Ozawa[a,d] and Jun-ichi Sawada[a,e]

We performed comprehensive haplotyping of *ABCB1/MDR1* gene blocks using 49 genetic polymorphisms, including seven novel ones, obtained from 145 Japanese subjects. The *ABCB1/MDR1* gene was divided into four blocks (Blocks −1, 1, 2, and 3) based on linkage disequilibrium analysis of polymorphisms. Using an expectation-maximization based program, 1, 2, 8, and 3 haplotype groups (3, 12, 32, and 18 haplotypes) were identified in Blocks −1, 1, 2, and 3, respectively. Within Block 2, haplotype groups *1, *2, *4, *6, and *8 reported by Kim and colleagues (*Clin Pharmacol Ther* 2001; 70:189–199) were found, and additional three groups (*9 to *11) were newly defined. We analyzed the association of haplotypes with the renal clearance of irinotecan and its metabolites in 49 Japanese cancer patients given irinotecan intravenously. There was a significant association of the *2 haplotype in Block 2, which includes 1236C>T, 2677G>T and 3435C>T, with a reduced renal clearance of those compounds. Moreover, tendencies of reduced and increased renal clearance were also observed with *1f in Block 2 and *1b in Block 3, respectively. These findings suggest that the P-glycoprotein encoded by *ABCB1/MDR1* in the proximal tubules plays a substantial role in renal exclusion of drugs and, moreover, that block-haplotyping is valuable for pharmacogenetic studies.
***Pharmacogenetics* 13:741–757 © 2003 Lippincott Williams & Wilkins**

Pharmacogenetics 2003, 13:741–757

Keywords: ABCB1, MDR1, P-glycoprotein, single nucleotide polymorphism, haplotype, renal clearance, irinotecan, SN-38

[a]Project Team for Pharmacogenetics, Divisions of [b]Xenobiotic Metabolism and Disposition, [c]Medicinal Safety Science, [d]Pharmacology, [e]Biochemistry and Immunochemistry, National Institute of Health Sciences, 1-18-1, Kamiyoga, Setagaya-ku, Tokyo 158-8501, Japan, Departments of [f]Cardiology, [g]Cardiovascular Dynamics, [h]Pharmacy, Research Institute, National Cardiovascular Center, Suita 565-8565, Japan, [i]Gastrointestinal Oncology Division and [j]Medical Oncology Division, National Cancer Center Hospital, [k]Genetics Division, National Cancer Center Research Institute, 5-1-1, Tsukiji, Chuo-ku, Tokyo 104-0045, Japan, Divisions of [l]Oncology/Hematology and [m]GI Oncology/Digestive Endoscopy, National Cancer Center Hospital East, 6-5-1, Kashiwanoha, Kashiwa 277-8577, Japan, [n]Division of Genomic Medicine, Department of Advanced Biomedical Engineering and Science, Tokyo Women's Medical University, 10-22 Kawada-cho, Shinjuku-ku, Tokyo 162-0054, Japan and [o]Safety Science Research Division, Mitsubishi Research Institute, Inc., 2-3-6 Otemachi, Chiyoda-ku, Tokyo 100-0004, Japan.

This study was supported in part by the Program for the Promotion of Fundamental Studies in Health Sciences (MPJ-1, MPJ-3 and MPJ-6) of the Organization for Pharmaceutical Safety and Research (OPSR) of Japan. Analytical standards of irinotecan and its metabolites were kindly supplied by Yakult Honsha Co. Ltd. (Tokyo, Japan).

Correspondence and requests for reprints to: Kimie Sai, PhD, Division of Xenobiotic Metabolism and Disposition, National Institute of Health Sciences, 1-18-1 Kamiyoga, Setagaya-ku, Tokyo 158-8501, Japan.
Tel: +81-3-3700-9478; fax: +81-3-3707-6950; e-mail: sai@nihs.go.jp

Received 12 May 2003
Accepted 19 August 2003

Introduction

P-glycoprotein (P-gp), a large transmembrane glycoprotein, was originally identified as a component of the multidrug resistance phenotype in cancer cells treated with a variety of lipophilic anti-tumor drugs such as colchicine, *Vinca* alkaloids, and anthracyclines [1,2]. P-gp is encoded by the *MDR1* gene [3], which is located on chromosome 7q21–q31 and consists of 28 exons [4]. This protein is also expressed in normal tissues, such as the brain, liver, kidneys, adrenals, and intestine [5,6], and is responsible for the outward transport of a wide variety of substrates including many drugs (usually hydrophobic or amphipathic compounds), utilizing ATP as an energy source [7]. Structural analysis of P-gp has revealed that it has two ATP-binding sites, and this protein is classified into the ATP-binding cassette (ABC) transporters [8], now termed ABCB1. In addition to a role for protecting tissues from intruding toxic xenobiotics, P-gp has been well-recognized as one of the important determinant molecules of drug responsiveness that may affect the pharmacokinetics of many drugs by counteracting their intestinal absorption and facilitating their biliary and renal excretion.

0960-314X © 2003 Lippincott Williams & Wilkins

DOI: 10.1097/01.fpc.0000054137.14659.f7

Since Hoffmeyer and colleagues first reported a functional polymorphism of the *ABCB1(MDR1)* gene that was related to altered P-gp expression and activity *in vivo* [9], a number of single nucleotide polymorphisms (SNPs) of this gene have been identified [10,11]. Kim and coworkers surveyed the exonic regions of *ABCB1* from 37 healthy European-Americans and 34 healthy African-Americans, and they found 10 new SNPs and classified 15 *ABCB1* haplotypes [12]. Subsequently, ethnically different haplotypic profiles in the *ABCB1* gene have been identified in three Asian populations [13].

Of these polymorphisms, much attention has been focused on the synonymous alteration of 3435C>T in exon 26, for which Hoffmeyer and colleagues showed reduced P-gp expression and activity [9]. Some studies supported their results [14,15], but several did not [12,16–18]. Possible functional alterations have also been shown for nonsynonymous polymorphisms 2677G>A and 2677G>T in exon 21 (Ala893Thr and Ala893Ser, respectively) and a combination of 2677G>T and 3435C>T [12,18]. However, the results reported so far are still controversial, as reviewed by Kim [19]. The reasons for these conflicting results are not yet clear. However, it is probable that there might be other unknown functional variations that are linked with these common SNPs. This prompted us to conduct comprehensive haplotype identification and classification, and to apply the obtained haplotypes for pharmacogenetic studies.

In our previous study, we sequenced 28 exons and their flanking intronic regions of *ABCB1* for 60 Japanese subjects, and found 12 novel SNPs [20]. Here, we sequenced the same regions and an additional enhancer region [21] for a total of 145 subjects (an additional 85 patients) and analyzed their haplotype configurations. Then, we assessed the functional association of the haplotypes with pharmacokinetic parameters of irinotecan and its metabolites in 49 Japanese cancer patients who received intravenous infusion of irinotecan. Irinotecan (or CPT-11) is a water-soluble derivative of camptothecin, a plant alkaloid isolated from the Chinese tree, *Camptotheca acuminata*, and currently used in the treatment of many types of cancer. An active metabolite, SN-38, which acts as a topoisomerase inhibitor, is produced by carboxylesterase in the liver [22], small intestine [23], and plasma [24]. SN-38 is further conjugated via uridine diphosphate glucuronosyl transferase (UGT) 1A1 in the liver to yield SN-38G [25]. Another inactive metabolite, APC, is produced by cytochrome P450 3A4 [26]. P-gp is known to contribute to transport of irinotecan and, to a lesser extent, of SN-38 and SN-38G [27–31]. In the present study using pharmacokinetic data from 49 cancer patients given irinotecan, we identified *ABCB1* haplotypes responsible for altered renal clearance of irinotecan and its metabolites.

Materials and methods

Chemicals

Irinotecan (7-ethyl-10-[4-(1-piperidino)-1-piperidino]-carbonyloxycamptothecin: CPT-11), 7-ethyl-10-hydroxy-camptothecin (SN-38), SN-38 glucuronide (SN-38G), 7-ethyl-10-[4-*N*-(5-aminopentanoic acid)-1-piperidino]carbonyloxycamptothecin (APC) were kindly supplied by Yakult Honsha Co. Ltd. (Tokyo, Japan). (S)-(+)-Camptothecin (CPT) was purchased from Tokyo Kasei Co. Ltd. (Tokyo, Japan).

DNA samples

The 145 Japanese subjects in this study consist of 85 ventricular tachycardia patients who were given amiodarone, and 11 and 49 patients with various cancers who were given paclitaxel and irinotecan, respectively. DNA was extracted from blood leukocytes and used for DNA sequence analysis. The ethics committees of the National Cardiovascular Center, the National Cancer Center, and the National Institute of Health Sciences approved this study. Written informed consent was obtained from all participating subjects.

DNA sequencing

Sequence data for 60 arrhythmic patients described previously [20] were incorporated into the present study by additional sequencing of an enhancer region [21]. Additionally, the *ABCB1* gene was sequenced for 25 arrhythmic patients and 60 cancer patients. At first, all 28 exons and the enhancer region around −7 kb (from the 5′-end of exon 1) of *ABCB1* were amplified from genomic DNA (200 ng in a 100-μl reaction volume) using 2.5 units of Z-taq (Takara Bio Inc. Shiga, Japan) with 0.2 μM of 1st amplification primers (Table 1). The first PCR conditions consisted of 30 cycles of 98°C for 5 s, 55°C for 5 s, and 72°C for 190 s, using the GeneAmp PCR system 9700 (Perkin-Elmer Co. Shelton, CT). Then, the PCR products (100 μl) were amplified using 0.625 units of Ex-Taq (Takara Bio Inc., Shiga, Japan) with the 2nd amplification primers (0.5 μM each) (Table 1), followed by direct sequencing of both strands using sequencing primers (Table 1). The procedure and PCR conditions through the 2nd amplification to sequencing were the same as described previously [20].

Linkage disequilibrium (LD) and haplotype analyses

LD analysis was carried out using the program SNPAlyze 2.2 (Dynacom Co. Ltd., Yokohama, Japan), and a pairwise two-dimensional map between SNPs was obtained for the values of chi square and rho square. All of the allele frequencies were in the Hardy–Weinberg equilibrium ($P > 0.15$, mostly higher than 0.9). Because both parameters were almost equivalent,

Table 1 Primers for amplification and sequencing of *ABCB1* exons

Exon	Primer name	Forward primer (5′ to 3′)	Primer name	Reverse primer (5′ to 3′)
First amplification (mixed primer)				
−7k to 3	MDR1-1ZF1	CCTGCTCTGTTTTTCACCGT	MDR1-1ZR1	ATTGGTTTCCTCTATGCAGA
3 to 4	MDR1-2ZF1	CATTTAGGACTCCAGACATT	MDR1-2ZR1	ATTCCTGCATCTACTTCCAG
5 to 9	MDR1-3ZF1	CCATACCAGTTGAAATCAGA	MDR1-3ZR1	TGCTATTGAGATTGCTAACG
10 to 20	MDR1-4ZF1	TCCTCACTTGACACCTTTTG	MDR1-4ZR1	ATTCTTAAAGAAGCCCCATA
21 to 23	MDR1-5ZF1	TCTGGTTTACAGTTGGACAT	MDR1-5ZR1	CTCTGACCGAGGTACAATTA
24 to 28	MDR1-6ZF1	CGGCTGGACTTACTCATGTG	MDR1-6ZR1	CACTTTATGCAAACATTTCA
Second amplification				
−7k	MDR1-1ZF2	GAGTGAATGAATGAGTTTCC	MDR1-7kR2	CTGTGCTTAGCAAATTATTC
1	MDR1-1F	CCCTTAACTACGTCCTGTAG	MDR1-1R	CGCCTCAAGAAGCCCTTCTC
2	MDR1-2F	TCTTACTGCTCTCTGGCTTC	MDR1-2R	CTCTAAGCAGGGATATTGAT
3	MDR1-3F	CACTCAGTGATAACCACGTA	MDR1-3R	CCCTATACGAAAATCTTACATC
4	MDR1-4F1	TAGCAAAGGTAGAGGGTGTC	MDR1-4R1	TGCTGGCACTTCAGTTGTGT
5	MDR1-5F	CACACAGTCAGCAGAGAAGT	MDR1-5R1S	AAAAGACTACCTTAAACTCCTC
6	MDR1-6F1	TGTTAAGGATGGCGAGATAC	MDR1-6R1	ACACCTCCTAACAGATGTGA
7	MDR1-7F	TCCTAGTAGAAACTTCTACC	MDR1-7R	TACAGAATCAGAGTCATCAT
8	MDR1-8F	ACCAAAGGCAAGTAAAAGAC	MDR1-8R1	GCCCATCTAGAAAACTCTTTG
9	MDR1-9F1	ATAGGGTCAATGTATGAGCA	MDR1-9R	CCACTTTTTAACCTAGTAGTGC
10	MDR1-10F	TATGTTGCCTCGCCATTTTA	MDR1-10R	AGTGATATTTTGTGGAGAGC
11	MDR1-11F	TCTTTGTCACTTTATCCAGC	MDR1-11R2	AGGACGAGTGAGAAAAAAAC
12	MDR1-12F3	AGAAGCCAAGTATTGACAGC	MDR1-12R2	CCTGTCCATCAACACTGACC
13	MDR1-13F4	TGGTTGGAAACAGTGGCTGT	MDR1-13R2	TTGATACTGCTAGAGCTTTC
14	MDR1-14F	TTGGGCTGTGTATAGGATTC	MDR1-14R	TGAAGGAATCACCTAGAAGC
15	MDR1-15F	CACAGCATTGGTTCAGTAAA	MDR1-15R	GGTGTTGTTTCCTACTTTGT
16	MDR1-16F	AAACAACACAGCAGATTAGC	MDR1-16R2	GACATTCTGGGGGATAGGAC
17	MDR1-17F2S	AAGCAAAATTGTCATCACTT	MDR1-17R1	TGATGACAAAGGAAGGTTCA
18	MDR1-18F	ATTTCCAGCGTACTAAGGCT	MDR1-18R	CAGAAAAACTTGGCTGTTAG
19	MDR1-19F	GTCACAGAAACATAGCAAGC	MDR1-19R	AGACTGAGGGACAACCAATA
20	MDR1-20F1	ACTTAGAAATCATGCGTAGG	MDR1-20R1	GCATGTGATATATTCGTAGG
21	MDR1-21F1	AGCATTCTGAAGTCATGGAA	MDR1-21R1	AGATTGCTTTGAGGAATGGT
22	MDR1-22F	CTACAGAGAAAATGCTCATACATAA	MDR1-22R	TAGCCAAAGTAATCCCTCTG
23	MDR1-23F	TGTGCCCTACTGCCAACCTA	MDR1-23R1	AGGAATCACCAGAATCTCTT
24	MDR1-24F1	TAAGCCCTGGAGATCATATC	MDR1-24R1	AGCAGTATTCCTATTTCCCT
25	MDR1-25F	CTTCTGACACCTGGTAATCG	MDR1-25R	GGCTCTCAGACTTTATCCAA
26	MDR1-26F	TTGGCAGTTTCAGTGTAAGA	MDR1-26R2	ACAACTAACCCAAACAGGAA
27	MDR1-27F1	CATGAACCATTCTTAGCTTC	MDR1-27R	ACTGTCAATAATCTGGCTGC
28	MDR1-28F2	CAAGCCCAGCTAATTTTTTG	MDR1-28R1	TCTGAACTTGACTGAGGAAA
Sequencing				
−7k	MDR1-1ZF2	GAGTGAATGAATGAGTTTCC	MDR1-7kR1	AAACCCTTTGCCCTAAGATA
1	MDR1-1F	CCCTTAACTACGTCCTGTAG	MDR1-1R	CGCCTCAAGAAGCCCTTCTC
2	MDR1-2F1	TACTGCTCTCTGGCTTCGAC	MDR1-2R1	GCTAGCTTGCGTTTCTTAAA
3	MDR1-3F	CACTCAGTGATAACCACGTA	MDR1-3R	CCCTATACGAAAATCTTACATC
4	MDR1-4F2	CAAAGGTAGAGGGTGTCTTG	MDR1-4R	TACAGGACTAAACACACTAATG
5	MDR1-5F1	GCCATAATGCTTACACACAA	MDR1-5R2S	TGTATACTTTATGCAGCCAAT
6	MDR1-6F	GGAATGAGTGGTCTCTTTGG	MDR1-6R2	ACCTCCTAACAGATGTGATG
7	MDR1-7F	TCCTAGTAGAAACTTCTACC	MDR1-7R	TACAGAATCAGAGTCATCAT
8	MDR1-8F	ACCAAAGGCAAGTAAAAGAC	MDR1-8R2	TCAATCTGAAGGGCATTTGA
9	MDR1-9F1	ATAGGGTCAATGTATGAGCA	MDR1-9R	CCACTTTTTAACCTAGTAGTGC
10	MDR1 10F	TATGTTGCCTCGCCATTTTA	MDR1-10R	AGTGATATTTTGTGGAGAGC
11	MDR1-11F	TCTTTGTCACTTTATCCAGC	MDR1-11R1	ACTTCAAGGCAATTCACAGA
12	MDR1-12F1	TACCCATCTCGAAAAGAAGT	MDR1-12R1	GTAATTGAAAGGGCAACATC
13	MDR1-13F3	CACAGAGGGGATGGTGAGATG	MDR1-13R1	ACTGCTAGAGCTTTCAAATC
14	MDR1-14F	TTGGGCTGTGTATAGGATTC	MDR1-14R	TGAAGGAATCACCTAGAAGC
15	MDR1-15F	CACAGCATTGGTTCAGTAAA	MDR1-15R	GGTGTTGTTTCCTACTTTGT
16	MDR1-16F	AAACAACACAGCAGATTAGC	MDR1-16R1	TCTGGATAACCTCTCTTGTT
17	MDR1-17F1S	TTCATTGATAAGGAATAAGG	MDR1-17R2	TCACAAAGTTAGCTCTCCTA
18	MDR1-18F	ATTTCCAGCGTACTAAGGCT	MDR1-18R	CAGAAAAACTTGGCTGTTAG
19	MDR1-19F	GTCACAGAAACATAGCAAGC	MDR1-19R	AGACTGAGGGACAACCAATA
20	MDR1-20F2	CAGGGGGTATAAGTATAAAC	MDR1-20R1	GCATGTGATATATTCGTAGG
21	MDR1-21F	CTCAATAAACTTACAAGTAGACCTT	MDR1-21R1	AGATTGCTTTGAGGAATGGT
22	MDR1-22F	CTACAGAGAAAATGCTCATACATAA	MDR1-22R	TAGCCAAAGTAATCCCTCTG
23	MDR1-23F1	ACTGCCAACCTATCAAAAGT	MDR1-23R4	AGGCTTCACAGTAGGGTTTC
24	MDR1-24FS	GAGTGTCAGCTTTCTAGCAT	MDR1-24RS	AGCAGTAATTGAAAGGAATC
25	MDR1-25F	CTTCTGACACCTGGTAATCG	MDR1-25R	GGCTCTCAGACTTTATCCAA
26	MDR1-26F	TTGGCAGTTTCAGTGTAAGA	MDR1-26R1	AGGGTGTGATTTGGTTGCTA
27	MDR1-27F1	CATGAACCATTCTTAGCTTC	MDR1-27R	ACTGTCAATAATCTGGCTGC
28	MDR1-28F5	ACTGTGGAGCTTTTTATGGA	MDR1-28R2S	GGAAATGTTAAACAGATACC

the value of rho square is presented in Fig. 1 with 10-graded blue color. Some of the haplotypes were unambiguous from subjects with homozygous SNPs at all sites or a heterozygous SNP at only one site. Separately, the diplotype configurations (combinations of haplotypes) were inferred by the LDSUPPORT software, which determines the posterior probability distribution of the diplotype configuration for each subject based on the estimated haplotype frequencies [32].

Administration of irinotecan and sample collection for pharmacokinetic study

The subjects who received irinotecan were 49 Japanese cancer patients (36 males and 13 females, 45–73 years of age) in the National Cancer Center Hospitals (Tokyo and Chiba, Japan), who had not previously received irinotecan-chemotherapy. Some subjects were also given other anticancer drugs, such as cisplatin, mitomycin C, or 5-fluorouracil. The eligibility criteria for irinotecan therapy were as follows: total bilirubin, 2 mg/dl; glutamic oxaloacetic transaminase, 105 IU/l; glutamic pyruvic transaminase, 120 IU/l; creatinine, 1.5 mg/dl; performance status, 0–2. Patients with infectious disease, diarrhea, leucopenia, ileus, biliary obstruction, interstitial pneumonia or lung fibrosis, excessive pleural effusion, or ascites fluid were excluded. Each patient received a single 90-min intravenous infusion at doses of 60–150 mg/m^2. Two ml of heparinized blood were collected before administration of irinotecan (predose), and at 0 min (end of infusion), 20 min, 1 h, 2 h, 4 h, 8 h, and 24 h after infusion. The plasma was separated by centrifugation and stored at −80°C. Urine was collected and pooled from 0 to 24 h after the infusion, and a 10-ml aliquot was stored at −80°C. Blood collection was unable to be carried out for one subject, and urine collection was not completed for five subjects. Therefore, the data from 48 and 44 subjects were used for the analysis of the area under the plasma concentration–time curve (AUC) and urinary recovery/renal clearance, respectively.

Fig. 1

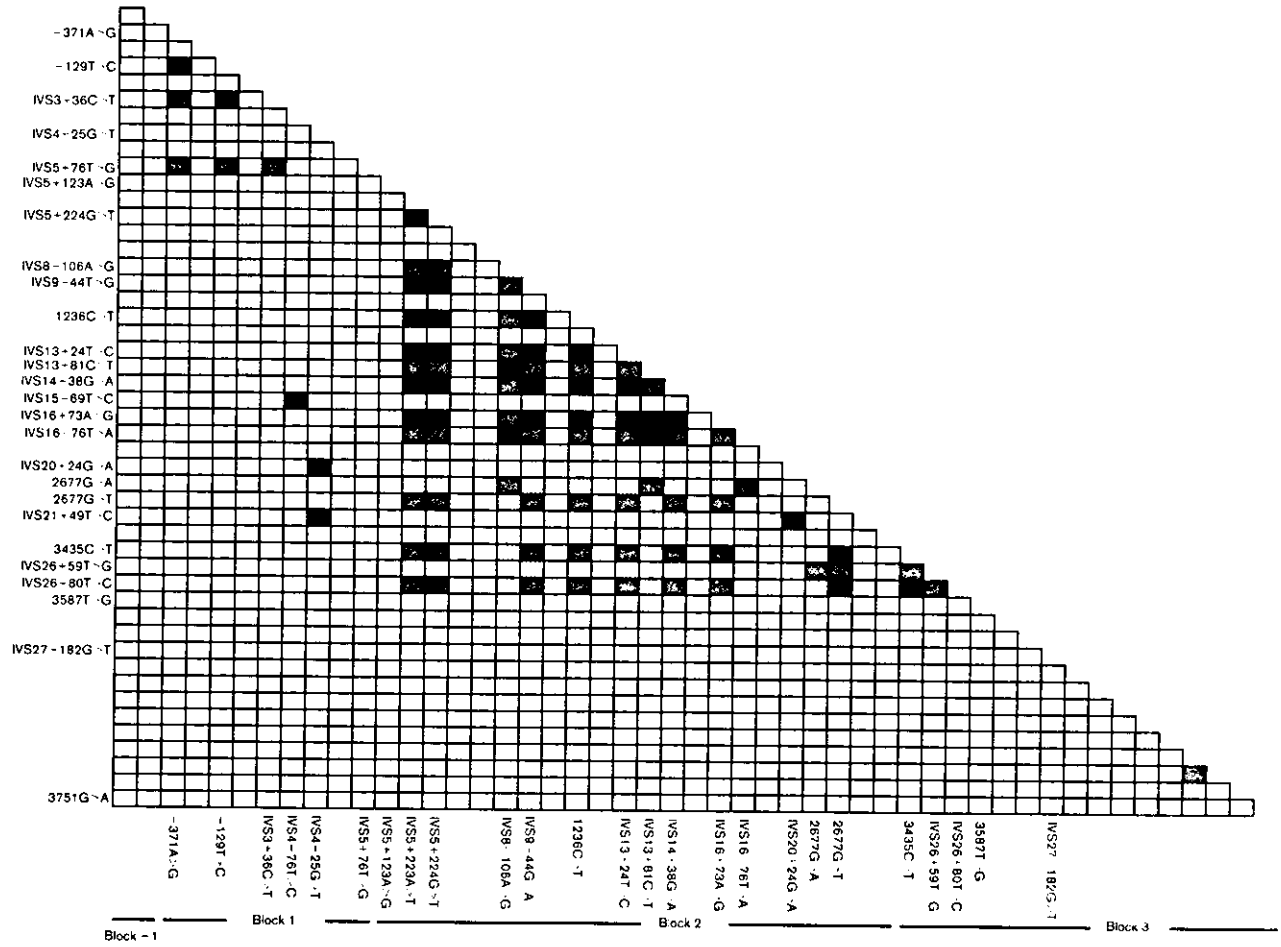

Linkage disequilibrium (LD) analysis for 49 *ABCB1* SNPs. Pairwise LD as ρ^2 (from 0 to 1) is expressed as 10-graded blue color. The more dense color represents the higher linkage.

Analysis of irinotecan and its metabolites

Concentrations of irinotecan, SN-38, SN-38G, and APC in the plasma and urine were determined by the HPLC method described previously [33]. One hundred μl of each urine sample was diluted with 900 μl of blank plasma. Two hundred-μl aliquots of the plasma or diluted urine were mixed with 200-μl aliquots of methanol/6% perchloric acid (1 : 1) containing 10 μl of camptothecin solution (internal standard) and mixed for 3 min, followed by centrifugation at 14 000 *g* for 3 min. The supernatant (200 μl) was mixed with 40 μl of 5 M ammonium acetate buffer (pH 4.5), and, after filtration, 100 μl of sample was injected into the HPLC system (HP 1100 model) equipped with a fluorescence detector (G1321A; (Hewlett Packard, Les Ulis, France). Chromatographic separation was performed using an analytical column CAPCELL PAK CN UG120, S-5 μm (4.6 mm i.d. × 150 mm; Shiseido, Co. Ltd., Tokyo, Japan) protected by a NewGuard C8 column (Perkin-Elmer Co., Norwalk, CT, USA) at a temperature of 40° C. The mobile phase for separation consisted of a mixture of acetonitrile : methanol : 0.05 M ammonium acetate (pH 4.5; 14 : 14 : 72) and was delivered at a flow rate of 0.5 ml/min. For fluorescence detection, the excitation wavelength was set at 368 nm, and the emission wavelengths were set at 432 nm for irinotecan, SN-38G, APC, and at 535 nm for SN-38. Detection and integration of chromatographic peaks were performed by the HP Chemistation data analysis system (Hewlett Packard).

Pharmacokinetic analysis

The AUCs of irinotecan and its metabolites were calculated by the linear trapezoidal rule using the WinNonlin ver.3.3 (Pharsight Corporation, Mountain View, CA, USA). The AUC (nmol/l h) from time zero to infinity (AUC_{inf}) was normalized by the administered dose of irinotecan (μmol/m^2). The renal clearance (l/h/m^2) was obtained by dividing the cumulative amount of each compound by the value of each AUC from zero to 24 h (AUC_{0-24h}).

Statistical analysis

All pharmacokinetic data in Tables 4 and 5 are presented as the mean ± standard deviation (SD). Statistical analysis of the difference in the mean values among genotypes was performed by analysis of variance followed by the Tukey–Kramer test using Prism, ver. 3.02 (GraphPad Software Inc., San Diego, CA, USA). The analysis of a trend of phenotype across the genotype was performed with the Jonckheere–Terpstra test in the SAS system, ver.5.0 (SAS Institute, Inc., Cary, NC, USA).

Results

SNPs detected in this study

Previously, we sequenced 28 exons (and their surrounding intronic regions) of the *ABCB1* gene of 60 Japanese arrhythmic patients and found 12 novel SNPs [20]. We have continued sequencing of the same and additional enhancer regions of *ABCB1* for a total of 145 patients. Novel SNPs and insertions found were −8104T>C, −7970C>T, IVS18-35G>C, 3587T>G, IVS27+63C>G, IVS27−86T>C, and IVS27−80insC, but their frequency was low (0.003 or 0.007). The SNP 3587T>G is non-synonymous (I1196S), and the other novel SNPs were intronic or 5′-flanking. An additional 31 reported SNPs were detected, and all SNPs found in this study are summarized in Table 2. In this Japanese population, we did not find the SNPs, −4C>T and −1G>A in exon 2, 548A>G in exon 7, 1474C>T in exon 13, 2650C>T in exon 21, and 3421T>A in exon 26, which have been used for classification of the *ABCB1* haplotypes *1B, *5, *1D, *2C, *2B, and *1C, respectively, by Kim and coworkers (Kim's haplotypes) [12] (Table 3). Thus, the frequencies of these SNPs are estimated to be less than (or around) 0.0034 (1/290) in the Japanese population. In contrast, the SNPs, 1236C>T (present in Kim's *2, *4, and *8), 2677G>T (present in Kim's *2, *3, and *7), and 3435C>T (present in Kim's *2, *3, *4, *5, and *6) were highly polymorphic in our study as well (Table 2). It is noteworthy that 2677G>A (0.200 = 58/290) and 2677G>T (0.403 = 117/290) are detectable at relatively high rates in the Japanese population.

Block assignment by LD analysis

The LD between 49 polymorphisms was analyzed pairwise for the values of chi square and rho square, and the data indicated that a very high LD was found in the region covering the two SNPs IVS5+123A>G and IVS26+80T>C. As for the values of chi square and rho square, the obtained results were almost equivalent, and the value of rho square is shown in Fig. 1. The four SNPs, −371A>G, −129T>C, IVS3+36C>T, and IVS5+76T>G, showed close associations with each other. A polymorphic alteration of IVS27−182G>T in exon 27 was not strongly associated with any SNPs (Fig. 1). From these findings, the *ABCB1* gene (the sequenced region spanned from 124732341 to 12367824 in NT_007793.10) was divided into four blocks: Block −1, approximately 7 kb upstream of the 5′-end of exon 1 including the PXR-binding region (the DR4 motif) [21]; Block 1, the 5′-flanking region of exon 1 (including −371A>G as a SNP) to the 3′-flanking of exon 5 (including IVS5+76T>G); Block 2, the 5′-flanking region of exon 6 (including IVS5+123A>G) to the 3′-flanking of exon 26 (including IVS26+80T>C); and Block 3, the 5′-flanking of exon 27 (including 3587T>G) to the 3′-untranslated region (including 3751G>A). Among 1176 SNP pairs, strong associations between the blocks were not found, except for the pairs of IVS15−69T>C and IVS4−76T>C, and for IVS4−25G>T, IVS20+24G>A, and IVS21+49T>C.

Table 2 List of SNPs and deletion/insertion of the *ABCB1* gene found in a Japanese population

Block	Site	SNP ID*			Position		Nucleotide change	Effect on protein	Frequency
		Our SNP ID	NCBI	IMS-JST	NT_007933.10	cDNA-based			
Block −1	5′-Flanking	MPJ6_AB1057			12472341	−8104	T>C		0.003
	5′-Flanking	MPJ6_AB1059			12472207	−7970	C>T		0.007
Block 1	5′-Flanking	MPJ6_AB1002	rs2188524	ssj0000008	12464608	−371	A>G		0.128
	Exon 1 (5′-UTR)	MPJ6_AB1003			12464382	−145	C>G		0.024
	Exon 1 (5′-UTR)	MPJ6_AB1004	rs3213619	ssj0000009	12464366	−129	T>C		0.093
	Intron 1	MPJ6_AB1005	rs3214119	ssj0000010	12463753	IVS1-74	delG		0.121
	Intron 3	MPJ6_AB1008	rs2235074		12459219	IVS3+36	C>T		0.093
	Intron 4	MPJ6_AB1010	rs2235014		12433788	IVS4-76	T>C		0.017
	Intron 4	MPJ6_AB1011	rs2235015		12433737	IVS4-25	G>T		0.086
	Exon 5	MPJ6_AB1012			12433674	325	G>A	E109K	0.010
	Intron 5	MPJ6_AB1013	rs2235016		12433585	IVS5+76	T>G		0.055
Block 2	Intron 5	MPJ6_AB1014	rs2235018		12433538	IVS5+123	A>G		0.141
	Intron 5	MPJ6_AB1015	rs2235020		12433438	IVS5+223	A>T		0.548
	Intron 5	MPJ6_AB1016	rs2235021		12433437	IVS5+224	G>T		0.548
	Intron 6	MPJ6_AB1017			12429839	IVS6-109	G>T		0.007
	Intron 7	MPJ6_AB1018			12429545	IVS7+14	G>A		0.010
	Intron 8	MPJ6_AB1020	rs1922240	ssj0000016	12417527	IVS8-106	A>G		0.348
	Intron 9	MPJ6_AB1021			12414371	IVS9-44	G>A		0.445
	Intron 10	MPJ6_AB1023	rs2235029		12414108	IVS10-41	T>G		0.017
	Exon 12	MPJ6_AB1025	rs1128503		12413774	1236	C>T	G412G (silent)	0.555
	Intron 12	MPJ6_AB1052			12413643	IVS12+17	G>A		0.010
	Intron 13	MPJ6_AB1026	rs2235033	ssj0000018	12413316	IVS13+24	T>C		0.445
	Intron 13	MPJ6_AB1027	rs2235035	ssj0000019	12413259	IVS13+81	C>T		0.348
	Intron 14	MPJ6_AB1028	rs2235013	ssj0000020	12412799	IVS14+38	G>A		0.445
	Intron 15	MPJ6_AB1029			12408557	IVS15-69	T>C		0.014
	Intron 16	MPJ6_AB1030	rs2235046		12408239	IVS16+73	A>G		0.452
	Intron 16	MPJ6_AB1031	rs1922242		12407840	IVS16-76	T>A		0.369
	Intron 18	MPJ6_AB1034			12402869	IVS18-35	G>C		0.003
	Intron 20	MPJ6_AB1035	rs2235040	ssj0000027	12399923	IVS20+24	G>A		0.090
	Exon 21	MPJ6_AB1036			12394791	2677	G>A	A893T	0.200
	Exon 21	MPJ6_AB1037	rs2032582		12394791	2677	G>T	A893S	0.403
	Intron 21	MPJ6_AB1038	rs2032583	ssj0000031	12394734	IVS21+49	T>C		0.090
	Intron 24	MPJ6_AB1040			12379982	IVS24+16	C>T		0.031
	Exon 26	MPJ6_AB1041	rs1045642	ssj0000040	12372818	3435	C>T	I1145I (silent)	0.441
	Intron 26	MPJ6_AB1042	rs2235047	ssj0000048	12372705	IVS26+59	T>G		0.403
	Intron 26	MPJ6_AB1043	rs2235048	ssj0000049	12372684	IVS26+80	T>C		0.448
Block 3	Exon 27	MPJ6_AB1068			12369435	3587	T>G	I1196S	0.003
	Intron 27	MPJ6_AB1044			12369323	IVS27+63	C>G		0.003
	Intron 27	MPJ6_AB1053			12368127	IVS27-189	A>G		0.007
	Intron 27	MPJ6_AB1045	rs1186745	ssj0000051	12369120	IVS27-182	G>T		0.200
	Intron 27	MPJ6_AB1054			12368110	IVS27-172	G>A		0.010
	Intron 27	MPJ6_AB1047	rs1186744		12368106	IVS27-168	T>C		0.010
	Intron 27	MPJ6_AB1048			12368105	IVS27-167	A>G		0.014
	Intron 27	MPJ6_AB1055			12368090	IVS27-152	A>G		0.003
	Intron 27	MPJ6_AB1049			12368057	IVS27-119	C>T		0.021
	Intron 27	MPJ6_AB1056	rs2235049		12368025	IVS27-87	A>G		0.007
	Intron 27	MPJ6_AB1070			12368024	IVS27-86	T>C		0.003
	Intron 27	MPJ6_AB1071			12368018	IVS27 80	ins C		0.003
	Exon 28	MPJ6_AB1051			12367824	3751	G>A	V1251I	0.010

*SNP ID assigned by our project team (MPJ-6).

Table 3 Classification of major *ABCB1* haplotypes

Site Position* Effect on protein	Exon 1 −4C>T	Exon 1 −1G>A	Exon 2 61A>G N21D	Exon 5 325G>A E109K	Exon 7 548A>G N183S	Exon 11 1199G>A S400N	Exon 12 1236C>T G412G	Exon 13 1474C>T R492C	Exon 21 2650C>T L884L	Exon 21 2677G>T A893S	Exon 21 2677G>A A893T	Exon 26 3421T>A S1141T	Exon 26 3435C>T I1145I	Exon 27 3587T>G I1196S	Exon 28 3751G>A V1251I
Classification by Kim *et al.* [12]															
*1	-	-	-		-	-	-	-	-	-		-	-		
*1A	-	-	-		-	A	-	-	-	-		-	-		
*1B	T	-	-		-	-	-	-	-	-		-	-		
*1C	-	-	-		-	-	-	-	-	-		A	-		
*1D	-	-	-		G	-	-	-	-	-		-	-		
*2	-	-	-		-	-	T	-	-	T		-	T		
*2A	-	-	G		-	-	T	-	-	T		-	T		
*2B	-	-	-		-	-	T	-	T	T		-	T		
*2C	-	-	-		-	-	T	T	-	T		-	T		
*3	-	-	-		-	-	-	-	-	T		-	T		
*4	-	-	-		-	-	T	-	-	-		-	T		
*5	-	A	-		-	-	-	-	-	-		-	T		
*6	-	-	-		-	-	-	-	-	-		-	T		
*7	-	-	-		-	-	-	-	-	T		-	-		
*8	-	-	-		-	-	T	-	-	-		-	-		
Classification of haplotype group detected in this paper**															
Block 1 *1	-	-	-	-											
*2	-	-	G	-											
Block 2 *1					-	-	-	-	-	-	-	-	-		
*2					-	-	T	-	-	T	-	-	T		
*4					-	-	T	-	-	-	-	-	T		
*6					-	-	-	-	-	-	-	-	T		
*8					-	-	T	-	-	-	-	-	-		
*9					-	-	-	-	-	-	-	-	-		
*10					-	-	-	-	-	-	A	-	-		
*11					-	-	T	-	-	-	A	-	-		
Block 3 *1														-	-
*2														-	A
*3														G	-

*Adenine of the initiation codon ATG in exon 2 was numbered +1.

**Major exonic SNPs in each haplotype group are shown in this table (Block −1 is not shown). Kim's haplotype groups of *3, *5, and *7 [12] were not detected, but an additional three haplotype groups of *9, *10, and *11 were newly defined in this study. Details on all haplotypes defined in this study are shown in Figs. 2 to 4.

Identification and classification of *ABCB1* haplotypes

We next attempted to utilize these SNPs for haplotyping the patient's *ABCB1* gene, as described by Kim and colleagues [12] (see Table 3). Kim's reported haplotypes *1, *2, *4, *6, and *8 were found within Block 2, and this previous classification of these haplotype groups was also used in this paper to avoid confusion. Haplotypes in a group were further specified with small letters. Without the aid of a computer program, some of the haplotypes were unambiguously assignable. However, haplotype combinations (diplotypes) of the subjects in the four blocks were confirmed or estimated by use of the LDSUPPORT program. The values of probability for most diplotypes were more than 0.99. The diplotypes with probability less than 0.99 are shown by adding '?' in Figs 2–4*. At least 1, 2, 8, and 3 haplotype groups were identified in Block −1, Block 1, Block 2, and Block 3, respectively (Table 3 and Figs 2–4).

Because the SNPs −8104T>C and −7970C>T are very distant from exon 1 and very rare, these two SNPs were separately analyzed as Block −1. In this block, the haplotypes *1a, *1b, and *1c were assigned (Fig. 2).

In Block 1, a haplotype having both a nonsynonymous SNP 325G>A (E109K) [34] and an intronic SNP IVS1-74delG was defined as *2. The *1 group haplotypes, *1a to *1j, and the *2 group haplotypes, *2a and *2b, were assigned with 9 SNPs (Fig. 2). The numbers of diplotypes and haplotypes are also shown in Fig. 2, and the haplotype *1a was found to be dominant.

Block 2 includes 25 SNPs and consists of the most complex haplotypes, as shown in Fig. 3. The wild-type haplotype (*1) always showed four intronic alterations: IVS9−44G>A, IVS13+24T>C, IVS14+38G>A, and IVS16+73A>G. Regarding the *1 group, Kim's haplotypes *1A,*1B, *1C, and *1D (Table 3) were not found, but 7 haplotypes, *1e to *1k, were newly identified (Fig. 3). The *1e haplotype is dominant among the *1 haplotype group. Kim's *2B, *2C, and

Fig. 2

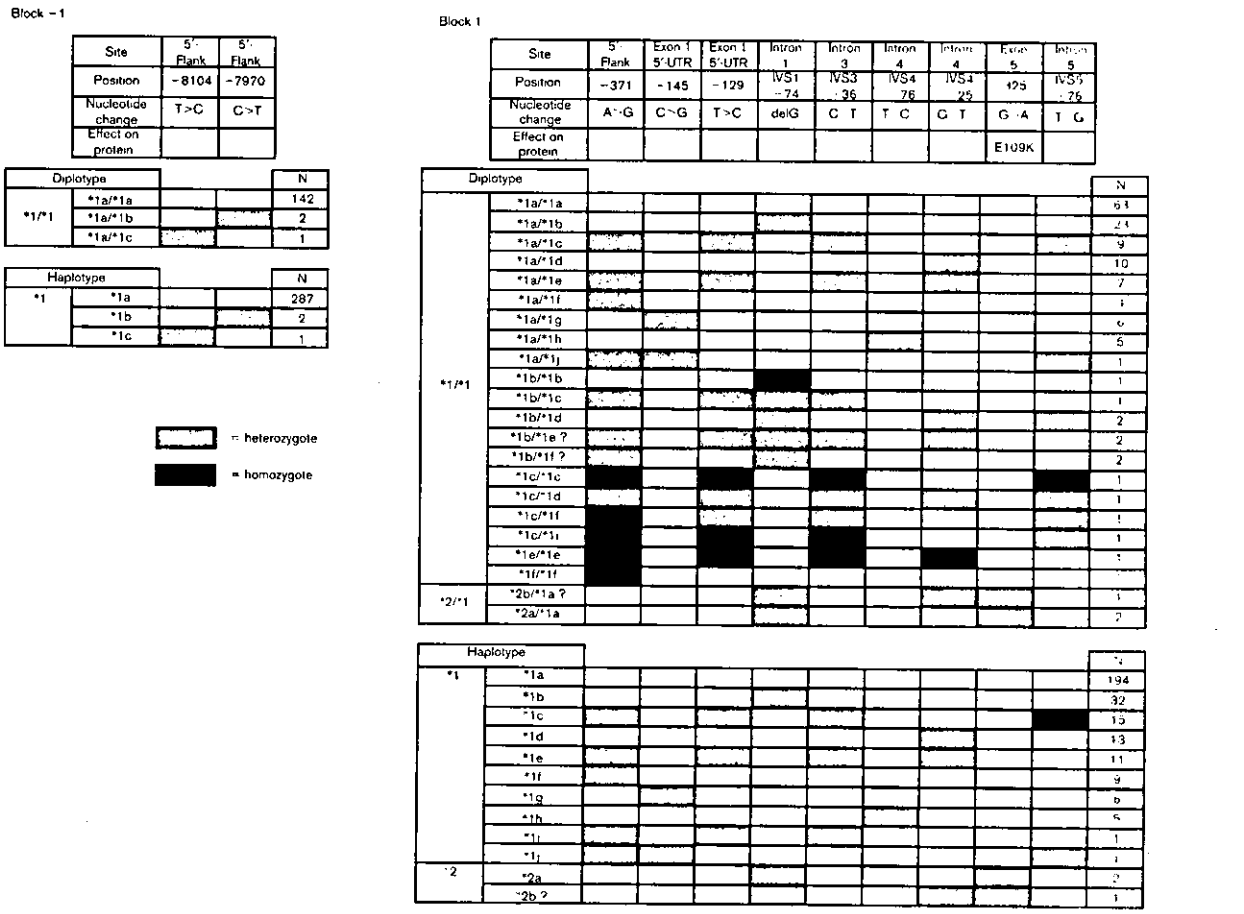

The diplotypes and haplotypes in Block −1 and Block 1 of the *ABCB1* gene for 145 Japanese subjects. The haplotypes assigned are described with small letters.

Fig. 3

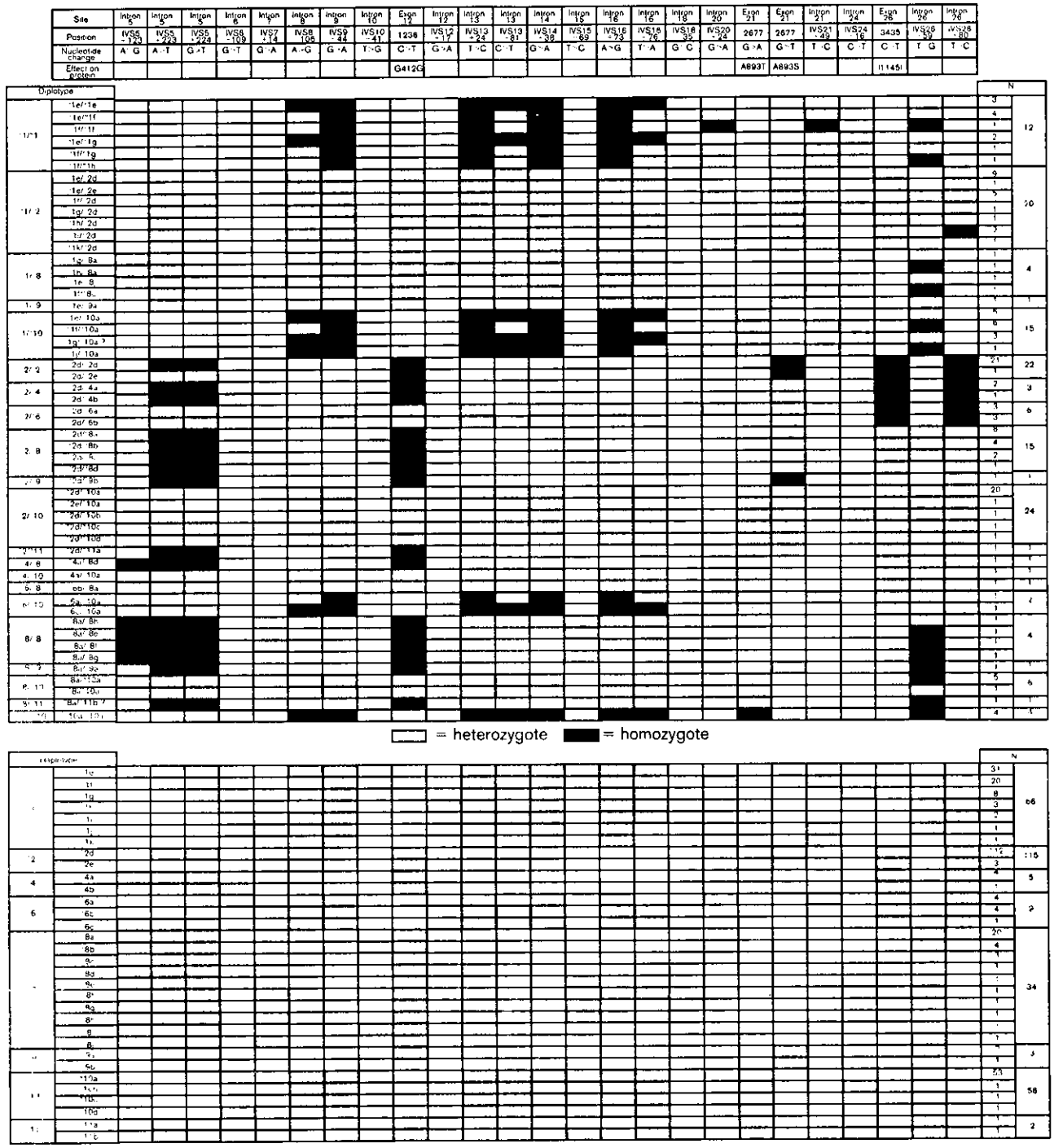

The diplotypes and haplotypes in Block 2 of the *ABCB1* gene for 145 Japanese subjects. Kim's haplotype groups of *3, *5, and *7 [12] were not detected in this study, and three novel haplotype groups of *9, *10, and *11 were defined. The haplotypes assigned are described with small letters.

*3 were not found, but *2d and *2e were newly identified. In the *2 group, *2d, which was dominant in Block 2, had IVS5+223A>T, IVS5+224G>T, and IVS26+80T>C, in addition to its marker SNPs, 1236C>T, 2677G>T, and 3435C>T. The *4 haplotypes showed IVS5+123A>G, IVS5+223A>T, IVS5+224G>T, and IVS26+80T>C, in addition to the marker SNPs, 1236C>T and 3435C>T. Kim's *5 haplo-

Fig. 4

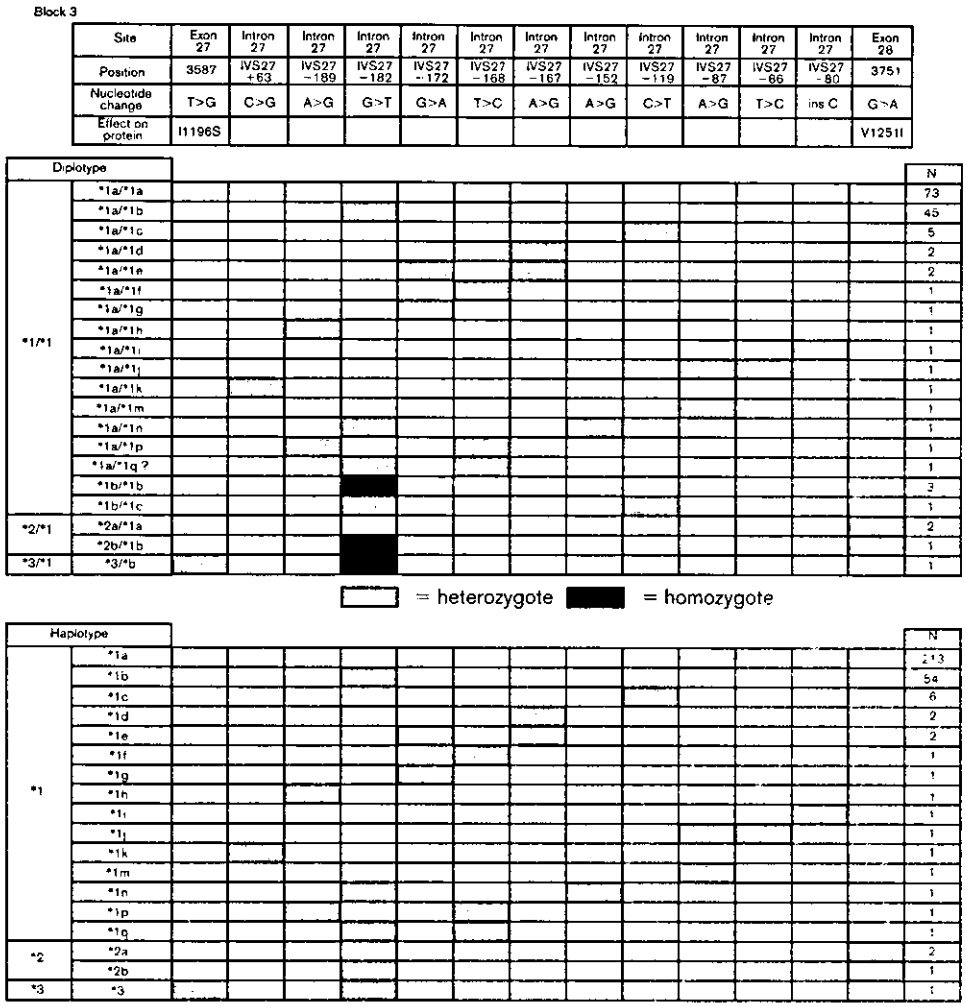

The diplotypes and haplotypes in Block 3 of the *ABCB1* gene for 145 Japanese subjects. The haplotypes assigned are described with small letters.

type is included in *6 in our definition (*6 plus −1G>A in Block 1), but it is not found in Japanese patients. The *6 haplotype having 3435C>T without 1236C>T and 2677G>T is relatively rare and classified into the three haplotypes *6a, *6b, and *6c. The *7 having 2677G>T without 1236C>T and 3435C>T was not found. The *8 haplotype with IVS5+123A>G, IVS5+223A>T, IVS5+224G>T, and IVS25+59T>G, in addition to its marker SNP 1236C>T, is still polymorphic within this group, and the ten haplotypes, *8a to *8j, were defined. We found the presence of a new haplotype with 1236C>T and 2677G>T but not 3435C>T in only three patients and named this haplotype *9. In addition, we defined the group of *10 for one of the major haplotypes having 2677G>A (A893T) in addition to the four *1 intronic SNPs. Four haplotypes, *10a, *10b, *10c, and *10d, were identified, but *10b, *10c, and *10d were very rare. Another novel haplotype, *11 (1236 C>T and 2677G>A), was newly defined, but *11a and *11b haplotypes were found in only one patient, respectively. As shown in Fig. 3, the haplotype groups *1, *2, *8, and *10 were major.

As for Block 3, *1 (*1a to *1q), *2 (*2a and *2b), and *3 were defined (Fig. 4). *1a and *1b were frequently found, and the other haplotypes were rare. The *2 and *3 haplotypes had a nonsynonymous SNP of 3751G>A (V1251I) and 3587T>G (I1196S), respectively.

Diplotypes in each block are also shown in Figs 2–4. In Block 1, the diplotypes, *1a/*1a and *1a/*1b are frequent (Fig. 2). In Block 2, diplotypes are very divergent, but the *1/*1, *1/*2, *1/*10, *2/*2, *2/*8, and *2/*10 diplotypes were relatively frequent. The *4, *6, *9, and *11 heterozygotes were found only in a small number of patients (Fig. 3). In Block 3, the diplotypes *1a/*1a and *1a/*1b were major (Fig. 4).

When the combinations of haplotypes in the four blocks were considered, the number of whole gene haplotypes (combinations like *1a–*1a–*1e–*1a (Block −1–Block 1–Block 2–Block 3), *1a–*1e–*1e–*1b, etc.) were too heterogeneous for association analysis. Notable exceptions were that the *1d or *1e in Block 1 was closely associated with the *1f in Block 2.

Haplotype-dependent difference in renal clearances of irinotecan and its metabolites

To clarify whether any haplotypes in the four blocks are responsible for functional alterations of P-gp, we investigated the relationship between the *ABCB1* genotypes described above and the pharmacokinetics of patients given irinotecan intravenously. We confirmed that the diplotype profiles of 49 patients on irinotecan were similar to those of the 145 subjects, except for a relatively small number of homozygotes of *2 in Block 2 (2/49). We first examined on Block 2, because haplotype *2 in Block 2 includes several marker SNPs, such as 1236C>T, 2677G>T, and 3435C>T, on which functional significance was reported. The mean values of AUC_{inf} of irinotecan and its metabolites among the genotypes were not significantly different. However, we found that the urinary excretion for 24 h (urinary recovery) of all of the compounds showed lower mean values in patients with the *2 haplotype. Therefore, we carefully investigated the genotype-dependency of renal clearance in all four blocks to identify the haplotypes affecting P-gp function.

In Block −1, we found that the values of various parameters for the *1b and *1c haplotypes were not considerably different from those of the *1a haplotype (data not shown). The individual values of renal clearance are plotted for the diplotypes in Blocks 1 to 3 (Figs 5–8). In Block 1, there were neither significant differences among the major diplotypes, *1a/*1a, *1a/*1b, and *1a/*1d, nor clear tendencies in minor genotypes ($n = 1$ or 2) for renal clearance values of all of the compounds (Fig. 5). Regarding Block 2, since the renal clearance values for patients having the *2 haplotype showed a decreasing tendency for all compounds, we divided all of the genotypes into the *2 haplotype and the non-*2 group, which includes the haplotypes of *1, *4, *6, *8, *9, and *10, based on the following findings (Fig. 6). With respect to *10 (2677G>A), the mean values of renal clearance of all compounds are not significantly different among the subjects of *1/*1, *10/*1, and *10/*10, or *1/*2 and *10/*2. Patients heterozygous for *6 (3435C>T) (*2/*6 ($n = 5$)) showed no significant difference in mean renal clearance values of all of the compounds from patients of *2/*1 ($n = 9$). In the case of the *8 haplotype (1236C>T), there was no significant difference in the mean values among the genotypes of *1/*1 ($n = 5$), *1/*8 ($n = 1$), *4/*8 ($n = 1$), and *8/*8 ($n = 2$). The very low frequencies of

Fig. 5

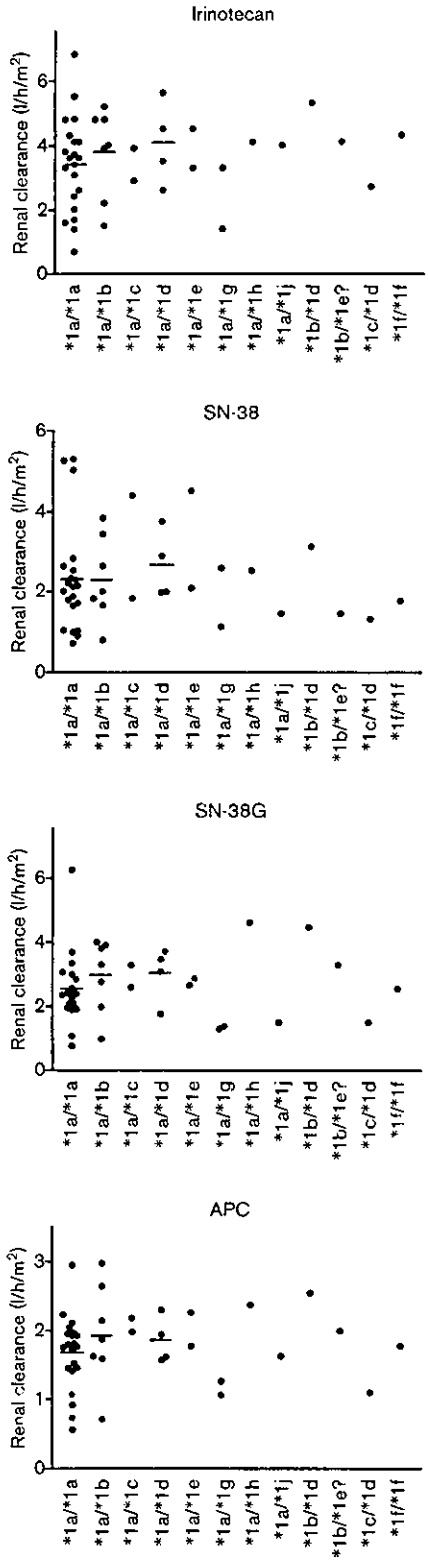

The relationship of the renal clearance of irinotecan and its metabolites to the genotypes in Block 1 of the *ABCB1* gene for Japanese cancer patients. Each point represents an individual, and the mean value in each genotype is shown as the bar (when $n \geq 3$).

Fig. 6

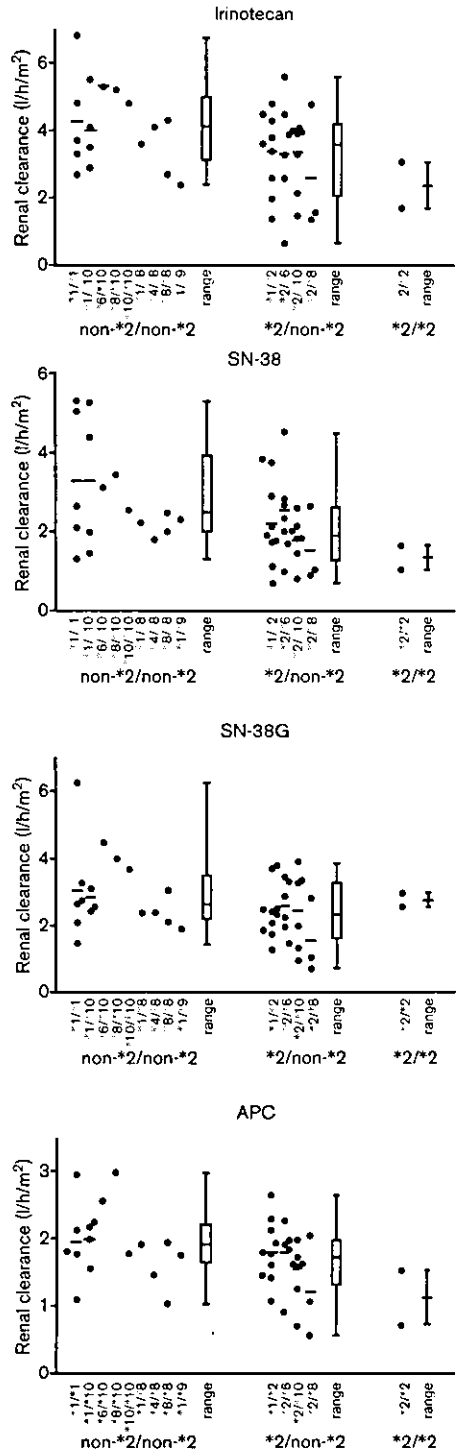

The relationship of the renal clearance of irinotecan and its metabolites to the genotypes in Block 2 of the *ABCB1* gene for Japanese cancer patients. Each point represents an individual, and the mean value in each genotype is shown as the bar (when $n \geq 3$). All genotypes were divided into non-*2/non-*2, *2/non-*2 and *2/*2 groups, and the distribution of each group was shown by the boxes representing 25th to 75th percentiles with a line at the median, and by bars representing the highest and lowest values. Statistical analysis for *2-dependency is summarized in Table 4.

Fig. 7

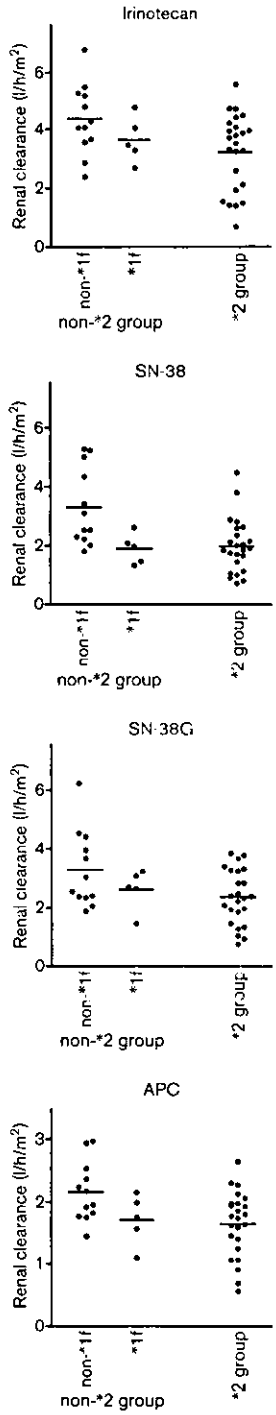

The relationship of the renal clearance of irinotecan and its metabolites to the genotype groups in *1f and *2 of Block 2 of the *ABCB1* gene for Japanese cancer patients. All genotypes (except for *1f/*2 and *2/*2) were divided into *2 (heterozygote) and non-*2 groups, and the non-*2 group was further divided into the *1f (heterozygote) and non-*1f groups. Each point represents an individual, and the mean value in each genotype group is shown as the bar (when $n \geq 3$). A statistically significant difference from the non-*1f group was detected for SN-38 ($P < 0.05$) in the *1f (heterozygote) group, and for irinotecan ($P < 0.05$), SN-38 ($P < 0.01$), SN-38G ($P < 0.05$), and APC ($P < 0.05$) in the *2 (heterozygote) group (Tukey–Kramer test).

Fig. 8

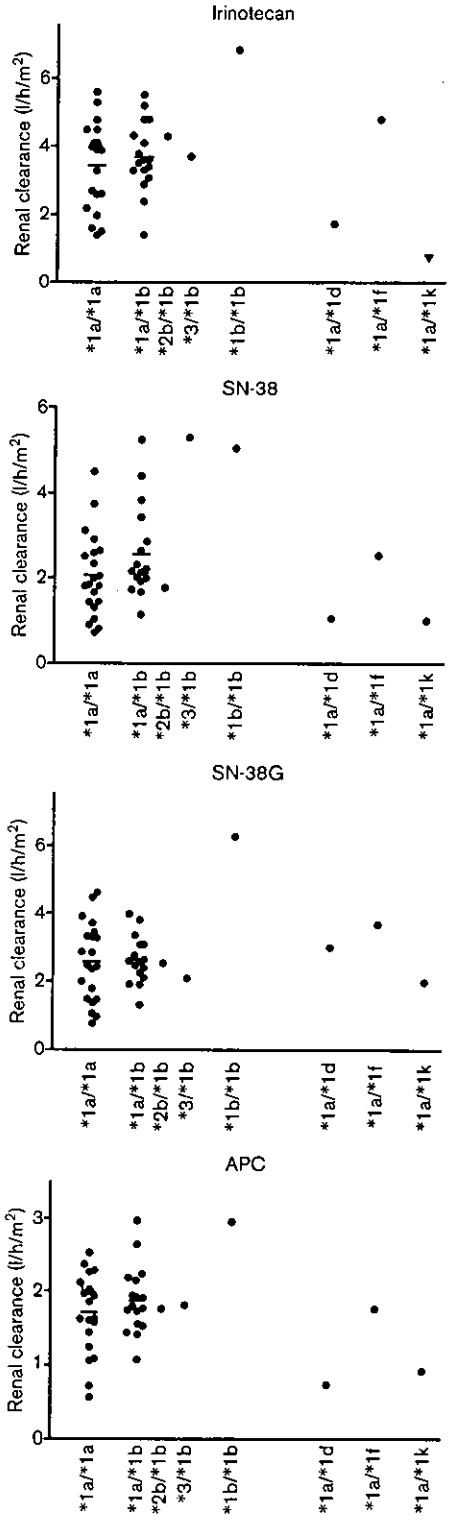

The relationship of the renal clearance of irinotecan and its metabolites to the genotypes in Block 3 of the *ABCB1* gene for Japanese cancer patients. Each point represents an individual, and the mean value in each genotype group is shown as the bar (when $n \geq 3$). The *1b-dependent increase was significant in SN-38 ($P < 0.05$, Jonckheere–Terpstra test).

*4 (1266C>T and 3435C>T) and *9 (2677G>T) heterozygotes made it difficult to assess their influence. However, since those two haplotypes do not have all three marker SNPs of *2, they are classified tentatively as the non-*2 group in this study.

We also carefully examined the effect of *1f in Block 2, which is linked with *1d or *1e in Block 1, on renal clearance and compared it with that of the *2 group. Notably, there are five subjects heterozygous for *1f in non-*2 group, and the renal clearance in these subjects showed a lower tendency for all of the compounds among the non-*2 group (Fig 7). A statistically significant reduction of the mean value in the *1f group compared with the non-*1f group was revealed in SN-38 ($P < 0.05$, using the Tukey–Kramer test); meanwhile, the statistical significance was much more evident in the *2 group for all of the compounds ($P < 0.05$ for irinotecan, SN-38G and APC, $P < 0.01$ for SN-38, using the Tukey–Kramer test). As we did not obtain data from homozygotes of *1f in this study, this decreasing trend should be clarified in a further study.

In the case of Block 3, we observed a slightly increasing tendency of the mean values for the patients with *1b in all of the compounds (Fig. 8). The increasing trend by *1b was statistically significant for SN-38 ($P = 0.0208$, using the Jonckheere–Terpstra test), but not for the others (Fig. 8). Regarding the patients with *1a/*1d and *1a/*1k, the values in irinotecan, SN-38 and APC were consistently much smaller than *1a/*1a. However, since these subjects belong to the *2 group in Block 2, a homozygote and a heterozygote, respectively, the *1d or *1k in Block 3 may not contribute to these lowered phenotypes.

From these findings, it was suggested that the *2 haplotype in Block 2 is the most effective for altering renal P-gp activity. A comparison of mean values for the AUC/dose, urinary recovery, and renal clearance among the groups of non-*2/non-*2, *2/non-*2, and *2/*2 in Block 2 is shown in Table 4. The value of AUC/dose in each compound was not significantly different among the genotypes. The urinary recovery values for all of the compounds decreased in a *2-dependent manner, and the value of irinotecan was statistically significant ($P = 0.0090$, using the Jonckheere–Terpstra test). Regarding the renal clearance, a *2-dependent decreasing tendency of the value was also evident in irinotecan, SN-38 and APC, giving P-values of 0.0154, 0.0043, and 0.0169, respectively (Table 4).

Because it is generally recognized that renal clearance is affected by many patient characteristics, such as age, weight, gender, or co-administered drugs, we examined whether those background factors might contribute to lower values of renal clearance in the *2-groups (Table

Table 4 Impact of the *ABCB1* haplotype *2 in Block 2 on the pharmacokinetics of irinotecan and its metabolites

Genotype group	AUC_{inf}/dose ($\times 10^{-3}$ h · m²/l)				Urinary recovery (%)				Renal clearance (l/hr/m²)			
	Irinotecan	SN-38	SN-38G	APC	Irinotecan	SN-38	SN-38G	APC	Irinotecan	SN-38	SN-38G	APC
Non-*2/non-*2[a] (n = 19)[c]	50.8 ± 18.3	2.55 ± 1.19	13.2 ± 7.07	9.11 ± 5.66	18.5 ± 3.97	0.464 ± 0.162	2.52 ± 1.12	1.61 ± 1.12	4.18 ± 1.14	2.90 ± 1.31	3.12 ± 1.18	2.03 ± 0.500
*2/non-*2[a,b] (n = 28)[d]	50.9 ± 16.8	2.81 ± 1.34	13.6 ± 7.55	8.98 ± 3.67	15.3 ± 5.88	0.382 ± 0.137	2.18 ± 0.948	1.28 ± 0.449	3.27 ± 1.29	2.06 ± 0.970	2.37 ± 0.931	1.65 ± 0.507
*2/*2[b] (n = 2)	50.9 ± 6.08	2.70 ± 1.32	9.17 ± 5.15	8.97 ± 5.50	12.0 ± 6.32	0.332 ± 0.289	2.07 ± 0.849	1.06 ± 1.08	2.39 ± 0.980	1.33 ± 0.433	2.77 ± 0.304	1.13 ± 0.564
P					< 0.01[e]				< 0.05[e]	< 0.01[e]		< 0.05[e]

Each value represents the mean ± SD. The values for renal clearance were obtained using the same data shown in Fig. 6.
[a]Non-*2 group includes *1, *4, *6, *8, *9, and *10 haplotypes.
[b]*2 group includes *2 haplotypes.
[c]Data for AUC and urinary recovery/renal clearance were not obtained for one and two subjects, respectively.
[d]Data for urinary recovery/renal clearance were not obtained for three subjects.
[e]Jonckheere–Terpstra test.

5). The mean values of age and weight were not significantly different between the groups of non-*2 and *2. Regarding the numbers of males and females, the numbers of females were much smaller than those of males in both the *2 and non-*2 groups. Then we checked the mean values of renal clearance in males and females separately. In the males, a significant *2-dependent decrease in the mean value was evident for all of the compounds. In the females, although the mean values of the non-*2-group were always smaller than those in the males, a *2-dependent decreasing tendency was still detected in the mean values of CPT-11 and APC (statistically not significant). Because the number of females in each group was small, it is difficult to evaluate gender differences in this study. However, this finding suggests a possibility that the expression levels of P-gp in the kidney might be lower in females, as in the case of the liver [35]. This would be clarified in a larger population, as planned in our future study. Regarding co-administered anticancer drugs, cisplatin was mainly given with irinotecan in this population (Table 5). We investigated the influence of cisplatin on the values of renal clearance in each group and found that no significant difference was obtained for all of the compounds between the subjects who received cisplatin and those who did not receive cisplatin (data not shown).

Discussion

To perform comprehensive haplotyping of *ABCB1*, we first divided the gene into four blocks based on LD analysis, and then haplotype combinations were determined. We defined 3 haplotypes in Block 1, 12 haplotypes in Block 2 (Fig. 2), 32 haplotypes of eight groups, including five previously reported haplotype groups, in Block 2 (Fig. 3), and 18 haplotypes in Block 3 (Fig. 4). As for Block 2, the reported haplotypes *1 to *8 by Kim and coworkers [12] were within this region, and we followed their previous classification and additionally assigned three novel haplotype groups, *9 to *11. Haplotype *2 includes the most common polymorphisms, 1236C>T, 2677G>T, and 3435C>T, which were also reported to be closely linked with each other. The frequencies of each polymorphism are 0.555, 0.200, 0.403, and 0.441, for 1236C>T, 2677G>A, 2677G>T, and 3435C>T, respectively. These frequencies were almost comparable with those obtained in the previous studies in the Japanese population [16,18,36] and an ethnic difference was also seen between our data and other Asian populations [13], Caucasians [11], and European-Americans or African-Americans [12].

Then, we investigated the relationship between the genotypes and the plasma concentration and renal excretion profiles of irinotecan and its metabolites in 49 cancer patients given irinotecan intravenously. Irinotecan and its metabolites are known to be excreted into

Table 5 Features of patients treated with irinotecan in each *2 haplotype group

Genotype group	Subject number		Age	Weight	Co-administered drugs			
	Male	Female	(years-old)	(kg)	Alone	Cisplatin	Mitomycin C	5-FU
Non-*2/non-*2[a] ($n = 19$)[c]	16	3	62.5 ± 7.69	62.4 ± 8.48	5	8	2	4
*2/non-*2[a,b] ($n = 28$)[d]	19	9	61.7 ± 7.17	55.8 ± 10.5	8	15	4	1
*2/*2[b] ($n = 2$)	1	1	63.5 ± 6.36	59.5 ± 11.7	1	1		

Each value represents the mean ± SD.
[a]Non-*2 group includes *1, *4, *6, *8, *9, and *10 haplotypes.
[b]*2 group includes *2 haplotypes.
[c]Data for AUC and urinary recovery/renal clearance were not obtained from one and two subjects, respectively.
[d]Data for urinary recovery/renal clearance were not obtained from three subjects.

both bile and urine, with an approximate ratio of 2 to 1 [37]. In-vivo studies using rats or mdr1a/1b knockout mice have indicated that irinotecan is excreted into the bile via P-gp located in the canalicular membrane in the liver [29,31]. Co-administration of cyclosporin, an inhibitor of P-gp, with intravenously administered irinotecan to rats caused an increase in the plasma concentration and a decrease in the systemic, renal, and non-renal clearance of irinotecan, and also caused a reduction in the urinary excretion of the metabolites SN-38 and SN-38G, although with to a lesser extent than irinotecan [27]. In-vitro studies also indicated that P-gp contributed to the transport of irinotecan and, to a lesser extent, of SN-38 [28,30]. SN-38G is also demonstrated to interact with P-gp, but its contribution for transport of SN-38G seemed smaller than for irinotecan [27,28].

The present study demonstrated that the block-haplotype analysis for *ABCB1* gene enabled identification of the haplotypes related to a decreased or increased function of P-gp, such as *2 or *1f in Block 2 or *1b in Block 3. This is also the first paper showing that the pharmacokinetics of irinotecan and its metabolites in patients can be affected by the *ABCB1* polymorphisms. A decreasing tendency for *1f in Block 2, which is linked with *1d or *1e in Block 1, was only identified in Block 2, but the analysis in Block 1 was unable to detect any trend for *1d or *1e due to a large diversity in the values for the wild-type (*1a/*1a in Block 1). This fact also indicates that the block-haplotype analysis could discriminate a responsible haplotype by changing the control group in each block.

Among those haplotypes, the *2 in Block 2 was most significantly associated with the phenotype for reduced renal clearance of irinotecan and its metabolites SN-38 and APC. Although the number of the *2-homozygotes was small, the *2-dependent reductions were clearly demonstrated (Fig. 6 and Table 4). In addition, the decreased renal clearance was also significant in the *2-heterozygotes as compared with the *1-group ($P < 0.01$ for CPT-11, $P < 0.05$ for SN-38, SN-38G and APC, Student's t-test) (data not shown). Thus the *2-haplotype may be one of the very critical factors for reduced function of P-gp. The fact that the effect of the *2 haplotype on renal clearance of SN-38G was relatively smaller might be attributed to a lower affinity of this compound for P-gp than irinotecan [27,28], and SN-38G might be preferentially transported by MRP2 [38]. Although APC has not been proven to be a P-gp substrate, our result suggests that P-gp may contribute to the excretion of APC as well as irinotecan and other metabolites. This apparent lowered activity of P-gp may result from reduced expression levels of P-gp in the renal proximal tubules, which is consistent with a previous report that the expression of P-gp in the kidney was significantly lower in a population with the polymorphisms of 3435T/T than that with 3435C/C [39].

Among the *1, *6, *8 and *10 groups in Block 2, no significant difference in renal clearance values was observed. Therefore, this finding implies that the activity of the P-gp variant with 1236C>T (*8), 2677G>A (Ala893Thr, *10), or 3435C>T (*6) alone is not altered. In the *2 haplotype, both 1236C>T and 2677G>T (Ala893Ser) are always linked with 3435C>T. This result suggests that 2677G>T alone or in combination with 1236C>T or/and 3435C>T in the *2 haplotype may be a causal genetic factor for decreasing P-gp activity.

Our finding is compatible with the report by Johne and colleagues, in which the plasma concentration of orally administered digoxin was revealed to be higher in subjects with both polymorphisms of 2677G>T and 3435C>T than in wild-type subjects [14]. Our observation is also consistent with the previous finding in Japanese volunteers on a significant reduction in the renal clearance of orally or intravenously administered digoxin in subjects with both 2677G> T and 3435C>T [15].

In contrast to the results above, there are still conflicting reports showing an enhanced or unchanged functional phenotype for the haplotype with both 2677G>T and 3435C>T [12,17,18,40]. The reason for these contradictory findings is still unknown. As our LD analysis showed that there was not any strong LD

between the *2 haplotype in Block 2 and any of the other three blocks, it is possible that an unknown intronic alteration closely linked with *2 within Block 2 might be a causal factor for the reduced activity of P-gp. Another possible association of the haplotypes, such as *1f in Block 2 and *1b in Block 3, with the P-gp function should also be taken into account in future studies.

The AUCs of irinotecan and its metabolites were not significantly different between the groups of non-*2 and *2. This may be partly attributed to the intravenous administration route; meanwhile, the bioavailability after oral administration is largely affected by the P-gp function of an absorption barrier in the enterocytes [15]. It is uncertain whether the *2 haplotype might be a causal factor for induction of the severe adverse effects by irinotecan, such as diarrhea or leucopenia, because the AUCs of irinotecan and its metabolites in the *2-group were not significantly different from those of the non-*2 group. However, since drugs were shown to accumulate in the tissues of the mdr1a/1b knockout mice [41], there is a possibility that the concentrations of irinotecan and its metabolites in the P-gp expressing tissues, such as the liver, intestine, and bone marrow of the *2-subjects might be higher than those of the non-*2 subjects, which might cause the adverse effects. An investigation of the association between clinical outcome and this *ABCB1* polymorphism is on-going in a larger population of patients.

In conclusion, we identified a panel of haplotypes of the *ABCB1* gene in a Japanese population and found some haplotypes leading to altered function of P-gp. The haplotype most significantly associated with reduced function was *2 in Block 2, which includes 1236C>T, 2677G>T, and 3435C>T. Our results also suggest that the urinary excretion of P-gp substrates is a sensitive marker for evaluating the *ABCB1* polymorphism. Moreover, the current study also indicates the usefulness of block-haplotyping for pharmacogenetic studies.

Acknowledgments

We would like to thank Drs T Mogami and S. Kojima for their generous support of our study, and Ms Chie Knudsen for her secretarial assistance.

References

1 Riordan JR, Deuchars K, Kartner N, Alon N, Trent J, Ling V. Amplification of P-glycoprotein genes in multidrug-resistant mammalian cell lines. *Nature* 1985; **316**:817–819.
2 Kartner N, Evernden-Porelle D, Bradley G, Ling V. Detection of P-glycoprotein in multidrug-resistant cell lines by monoclonal antibodies. *Nature* 1985; **316**:820–823.
3 Shen DW, Fojo A, Chin JE, Roninson IB, Richert N, Pastan I. *et al.* Human multidrug-resistant cell lines: increased mdr1 expression can precede gene amplification. *Science* 1986; **232**:643–645.
4 Trent JM, Witkowski CM. Clarification of the chromosomal assignment of the human P-glycoprotein/mdr1 gene: possible coincidence with the cystic fibrosis and c-met oncogene. *Cancer Genet Cytogenet* 1987; **26**:187–190.
5 Fojo AT, Ueda K, Slamon DJ, Poplack DG, Gottesman MM, Pastan I. Expression of a multidrug-resistance gene in human tumors and tissues. *Proc Natl Acad Sci U S A* 1987; **84**:265–269.
6 Cordon-Cardo C, O'Brien JP, Casals D, Rittman-Grauer L, Biedler JL, Melamed MR, *et al.* Multidrug-resistance gene (P-glycoprotein) is expressed by endothelial cells at blood-brain barrier sites. *Proc Natl Acad Sci U S A* 1989; **86**:695–698.
7 Horio M, Gottesman MM, Pastan I. ATP-dependent transport of vinblastine in vesicles from human multidrug-resistant cells. *Proc Natl Acad Sci USA* 1988; **85**:3580–3584.
8 Cole SP, Bhardwaj G, Gerlach JH, Mackie JE, Grant CE, Almquist KC, *et al.* Overexpression of a transporter gene in a multidrug-resistant human lung cancer cell line. *Science* 1992; **258**:1650–1654.
9 Hoffmeyer S, Burk O, von Richter O, Arnold HP, Brockmoller J, Johne A, *et al. Proc Nat. Acad Sci USA* 2000; **97**:3473–3478.
10 Brinkman U, Eichelbaum M. Polymorphisms in the ABC drug transporter gene MDR1. *Pharmacogenomics J* 2001; **1**:59–64.
11 Cascorbi I, Gerloff T, Johne A, Meisel C, Hoffmeyer S, Schwab M, *et al.* Frequency of single nucleotide polymorphisms in the P-glycoprotein drug transporter MDR1 gene in white subjects. *Clin Pharmacol Ther* 2001; **69**:169–174.
12 Kim RB, Leake BF, Choo EF, Dresser GK, Kubba SV, Schwarz UI, *et al.* Identification of functionally variant MDR1 alleles among European Americans and African Americans. *Clin Pharmacol Ther* 2001; **70**:189–199.
13 Tang K, Ngoi S-M, Gwee P-C, Chua JMZ, Lee EJD, Chong SS, *et al.* Distinct haplotype profiles and strong linkage disequilibrium at the MDR1 multidrug transporter gene locus in three ethnic Asian populations. *Pharmacogenetics* 2002; **12**:437–450
14 Johne A, Kopke K, Gerloff T, Mai I, Rietbrock S, Meisel C, *et al.* Modulation of steady-state kinetics of digoxin by haplotypes of the P-glycoprotein MDR1 gene. *Clin Pharmacol Ther* 2002; **72**:584–594.
15 Kurata Y, Ieiri I, Kimura M, Morita T, Irie S, Urae A, *et al.* Role of human MDR1 gene polymorphism in bioavailability and interaction of digoxin, a substrate of P-glycoprotein. *Clin Pharmacol Ther* 2002;**72**:209–219.
16 Tanabe M, Ieiri I, Nagata N, Inoue K, Ito S, Kanamori Y, *et al.* Expression of P-glycoprotein in human placenta: relation to genetic polymorphism of the multidrug resistance (MDR)-1 gene. *J Pharmacol Exp Ther* 2001; **297**:1137–1143.
17 Moriya Y, Nakamura T, Horinouchi M, Sakaeda T, Tamura T, Aoyama N, *et al.* Effects of polymorphisms of MDR1, MRP1, and MRP2 genes on their mRNA expression levels in duodenal enterocytes of healthy Japanese subjects. *Biol Pharm Bull* 2002; **25**:1356–1359.
18 Sakaeda T, Nakamura T, Horinouchi M, Kakumoto M, Ohmoto N, Sakai T, *et al.* MDR1 genotype-related pharmacokinetics of digoxin after single oral administration in healthy Japanese subjects. *Pharm Res* 2001; **18**:1400–1404.
19 Kim RB. MDR1 single nucleotide polymorphisms: multiplicity of haplotypes and functional consequences. *Pharmacogenetics* 2002; **12**: 425–427.
20 Itoda M, Saito Y, Komamura K, Ueno K, Kamakura S, Ozawa S, *et al.* Twelve novel single nucleotide polymorphisms in ABCB1/MDR1 among Japanese patients with ventricular tachycardia who were administered amiodarone. *Drug Metab Pharmacokinet* 2002; **17**:566–571.
21 Geick A, Eichelbaum M, Burk O. Nuclear receptor response elements mediate induction of intestinal MDR1 by rifampin. *J Biol Chem* 2001; **276**:14581–14587.
22 Slatter JG, Su P, Sams JP, Schaaf LJ, Wienkers LC. Bioactivation of the anticancer agent CPT-11 to SN-38 by human hepatic microsomal carboxylesterases and the in vitro assessment of potential drug interactions. *Drug Metab Dispos* 1997; **25**:1157–1164.
23 Khanna R, Morton CL, Danks MK, Potter PM. Proficient metabolism of irinotecan by a human intestinal carboxylesterase. *Cancer Res* 2000; **60**:4725–4728.
24 Kehrer DF, Yamamoto W, Verweij J, de Jonge MJ, de Bruijin P, Sparreboom A. Factors involved in prolongation of the terminal disposition phase of SN-38: clinical and experimental studies. *Clin Cancer Res* 2000; **6**:3451–3458.
25 Iyer L, King CD, Whitington PF, Green MD, Roy SK, Tephly TR, *et al.* Genetic predisposition to the metabolism of irinotecan (CPT-11). Role of uridine diphosphate glucuronosyltransferase isoform 1A1 in the glucuronidation of its active metabolite (SN-38) in human liver microsomes. *J Clin Invest* 1998; **15**:847–854.
26 Haaz MC, Rivory L, Riche C, Vernillet L, Robert J. Metabolism of irinotecan (CPT-11) by human hepatic microsomes: participation of

cytochrome P-450 3A and drug interactions. *Cancer Res* 1998; **58**:468–472.
27 Gupta E, Safa AR, Wang X, Ratain MJ. Pharmacokinetic modulation of irinotecan and metabolites by cyclosporin A. *Cancer Res* 1996; **56**:1309–1314.
28 Chu XY, Suzuki H, Ueda K, Kato Y, Akiyama S, Sugiyama Y. Active efflux of CPT-11 and its metabolites in human KB-derived cell lines. *J Pharmacol Exp Ther* 1999; **288**:735–741.
29 Chu XY, Kato Y, Sugiyama Y. Possible involvement of P-glycoprotein in biliary excretion of CPT-11 in rats. *Drug Metab Dispos* 1999; **27**: 440–441.
30 Yamamoto W, Verweij J, de Bruijn P, de Jonge MJ, Takano H, Nishiyama M, *et al.* Active transepithelial transport of irinotecan (CPT-11) and its metabolites by human intestinal Caco-2 cells. *Anticancer Drugs* 2001; **12**:419–432.
31 Iyer L, Ramirez J, Shepard DR, Bingham CM, Hossfeld DK, Ratain MJ, *et al.* Biliary transport of irinotecan and metabolites in normal and P-glycoprotein-deficient mice. *Cancer Chemother Pharmacol* 2002; **49**:336–341.
32 Kitamura Y, Moriguchi M, Kaneko H, Morisaki H, Morisaki T, Toyama K, *et al.* Determination of probability distribution of diplotype configuration (*diplotype distribution*) for each subject from genotypic data using the EM algorithm. *Ann Hum Genet* 2002; **66**:183–193.
33 Sai K, Kaniwa N, Ozawa S, Sawada J. An analytical method for irinotecan (CPT-11) and its metabolites using a high-performance liquid chromatography: parallel detection with fluorescence and mass spectrometry. *Biomed Chromatogr* 2002; **16**:209–218.
34 Honda T, Dan Y, Koyabu N, Ieiri I, Otsubo K, Higuchi S, *et al.* Polymorphisms of MDR1 gene in healthy Japanese subjects: A novel SNP with an amino acid substitution (Glu108Lys). *Drug Metab Pharmacokinet* 2002; **17**:479–481.
35 Schuetz EG, Furuya KN, Schuetz JD. Interindividual variation in expression of P-glycoprotein in normal human liver and secondary hepatic neoplasms. *J Pharmacol Exp Ther* 1995; **275**:1011–1018.
36 Ito S, Ieiri I, Tanabe M, Suzuki A, Higuchi S, Otsubo K. Polymorphism of the ABC transporter genes, MDR1, MRP1 and MRP2/cMOAT, in healthy Japanese subjects. *Pharmacogenetics* 2001; **11**:175–184.
37 Slatter JG, Schaaf LJ, Sames JP, Feenstra KL, Johnson MG, Bombardt PA, *et al.* Pharmacokinetics, metabolism, and excretion of irinotecan (CPT-11) following I.V infusion of [14C]CPT-11 in cancer patients. *Drug Metab Dispos* 2000; **28**:423–433.
38 Chu XY, Kato Y, Niinuma K, Sudo KI, Hakusui H, Sugiyama Y. Multispecific organic anion transporter is responsible for the biliary excretion of the camptothecin derivative irinotecan and its metabolites in rats. *J Pharmacol Exp Ther* 1997; **281**:304–314.
39 Siegsmund M, Brinkmann U, Schaffeler E, Weirich G, Schwab M, Eichelbaum M, *et al.* Association of the P-glycoprotein transporter MDR1(C3435T) polymorphism with the susceptibility to renal epithelial tumors. *J Am Soc Nephrol* 2002; **13**:1847–1854.
40 Kimchi-Sarfaty C, Gribar JJ, Gottesman MM. Functional characterization of coding polymorphisms in the human MDR1 gene using a vaccinia virus expression system. *Mol Pharmacol* 2002; **62**:1–6.
41 Cox DS, Scott KR, Gao H, Eddington ND. Effect of P-glycoprotein on the pharmacokinetics and tissue distribution of enaminone anticonvulsants: analysis by population and physiological approaches. *J Pharmacol Exp Ther* 2002; **302**:1096–1104.